

A Stability Analysis of the Fundamental Matrix

Q.-T. Luong^{1,2} and O.D. Faugeras¹

¹ INRIA, 2004 Route des Lucioles, 06561 Sophia-Antipolis, France

² EECS, Cory Hall 211-215, University of California, Berkeley, CA 94720, USA

Abstract. The *Fundamental matrix* is a key concept when working with uncalibrated images and multiple viewpoints. It contains all the available geometric information and enables to recover the epipolar geometry from uncalibrated perspective views. This paper is about a stability analysis for the Fundamental matrix. We first present a probabilistic approach which works well. This approach, however, does not give insight into the causes of instability. Two complementary explanations for instability are the nature of the motions, and the interaction between motion and three-dimensional structure, which is characterized by a *critical surface*. Practical methods to characterize the proximity to the critical surface from image measurements, by estimating a quadratic transformation, are developed. They are then used for experiments which validate our observations. It turns out that surprisingly enough, the critical surface affects the stability of the fundamental matrix in a significant number of situations.

1 Introduction

Inferring three-dimensional information from images taken from different viewpoints is a central problem in computer vision. However, since the measured data in images are just pixel coordinates, there are only two approaches that can be used in order to perform this task. The first one is to compute the model which relates pixel coordinates to a 3D reference coordinate system by camera calibration. Euclidean descriptions can then be obtained, but a significant amount of flexibility is lost to this procedure, which cannot be used practically an active system. Thus, a second approach is emerging [12], which consists in using projective geometry, whose non-metric nature allows to use uncalibrated cameras. These approaches use only geometric information which relates the different viewpoints. This information is entirely contained in the *Fundamental matrix*, thus it is very important to develop precise techniques to compute it, achieving thus a form of *weak calibration*. More recently, affine geometry has been found to provide an interesting framework borrowing some nice characteristics from both Euclidean geometry and projective geometry. Affine calibration also requires the determination of the fundamental matrix [14], [8].

A great deal of work has been devoted to the problem of characterizing the stability of estimation of Euclidean motion, however nothing has been done, to our knowledge, to characterize the stability of estimation of the fundamental matrix. This paper tries to shed some light on this important problem.

2 Characterizing the Fundamental Matrix Stability

The Projective Model The camera model which we consider is the pinhole model. The main property of this camera model is thus that *the relationship between the world coordinates and the pixel coordinates is linear projective*. This property is independent of the choice of the coordinate systems in the retinal plane or in the three-dimensional space. The consequence is that the relationship between 2-D pixel coordinates 3-D and any world coordinates can be described by a 3×4 matrix $\tilde{\mathbf{P}}$, called projection matrix, which maps points from \mathcal{P}^3 to \mathcal{P}^2 :

$$\begin{bmatrix} x_1 \\ x_2 \\ x_3 \end{bmatrix} = \tilde{\mathbf{P}} \begin{bmatrix} \mathcal{X}_1 \\ \mathcal{X}_2 \\ \mathcal{X}_3 \\ \mathcal{X}_4 \end{bmatrix} \quad (1)$$

where the retinal projective coordinates x_1, x_2, x_3 are related to usual pixel coordinates by $(u, v) = (x_1/x_3, x_2/x_3)$ and the projective world coordinates $\mathcal{X}_1, \mathcal{X}_2, \mathcal{X}_3, \mathcal{X}_4$ are related to usual affine world coordinates by $(X, Y, Z) = (\mathcal{X}_1/\mathcal{X}_4, \mathcal{X}_2/\mathcal{X}_4, \mathcal{X}_3/\mathcal{X}_4)$.

The Fundamental Matrix When considering two projective views, the main geometric property is known in computer vision as the epipolar constraint.

It can be shown only from the hypothesis (1) that the relationship between the projective retinal coordinates of a point \mathbf{m} and the projective coordinates of the corresponding epipolar line \mathbf{l}'_m is linear. The *fundamental matrix* describes this correspondence:

$$\begin{bmatrix} l'_1 \\ l'_2 \\ l'_3 \end{bmatrix} = \mathbf{l}'_m = \mathbf{F}\mathbf{m} = \mathbf{F} \begin{bmatrix} x_1 \\ x_2 \\ x_3 \end{bmatrix}$$

The epipolar constraint has then a very simple expression: since the point \mathbf{m}' corresponding to \mathbf{m} belongs to the line \mathbf{l}'_m by definition, it follows that

$$l'_1 x'_1 + l'_2 x'_2 + l'_3 x'_3 = \mathbf{m}'^T \mathbf{F}\mathbf{m} = 0 \quad (2)$$

This last equation is similar to Longuet-Higgins' equation relating the essential matrix [3], and *calibrated* coordinates. In particular, it is linear in the entries of \mathbf{F} .

Parameterizing the Fundamental Matrix The epipolar transformation is characterized by the 2×2 projective coordinates of the epipoles \mathbf{e} and \mathbf{e}' (which are defined respectively by $\mathbf{F}\mathbf{e} = 0$ and $\mathbf{F}^T \mathbf{e}' = 0$), and by the 4 coefficients a, b, c, d of the homography between the two pencils of epipolar lines. We have to find a parameterization for the pencils of epipolar lines such that the correspondence has a simple form. One solution, valid in the practical case where epipoles are at finite distance, consists in intersecting each epipolar line with the line at infinity, which consists of retinal points for which the third projective component is zero. The epipolar transformation can then be expressed as a collineation of this line. If the epipolar line l goes through the point \mathbf{m} , then its intersection with this line at infinity is $\mathbf{y}_\infty = (\mathbf{e} \times \mathbf{m}) \times (0, 0, 1)^T$, which can be written as $(1, \tau, 0)^T$, with:

$$\tau = \frac{m_2 - e_2}{m_1 - e_1} \quad (3)$$

If \mathbf{m}' corresponds to \mathbf{m} , then the epipolar line l' of the second image going through \mathbf{m}' corresponds to l . It is parameterized by the point $\mathbf{y}'_\infty = (1, \tau', 0)^T$, with its projective

parameter obtained by priming the quantities in (3). The epipolar transformation maps \mathbf{y}_∞ to \mathbf{y}'_∞ , and thus is an homographic function in the projective parameters:

$$\tau \mapsto \tau' = \frac{a\tau + b}{c\tau + d} \quad (4)$$

Epipoles Stability Characterize Fundamental Matrix Stability The estimation of the fundamental matrix can be done as a two-stage process, the first one being the estimation of the coordinates of the epipoles, and the second one the estimation of the coefficients of the homography. If one of the two stages is significantly more sensitive to noise than the other one, then we can conclude that its stability determines the stability of the overall estimation. Let us see that it is indeed the case, using a statistical simulation with variation of the 3D motion of the camera.

- The fundamental matrix has been computed from point correspondences using the quadratic criterion derived from the linear relation (2). The epipoles \mathbf{e} and \mathbf{e}' are then computed from this matrix [6].
- The coefficients of the epipolar homography have been computed from the point correspondences and the *correct* epipoles, using a linear least-squares formulation based on the relation derived by making substitutions of (3) in (4).

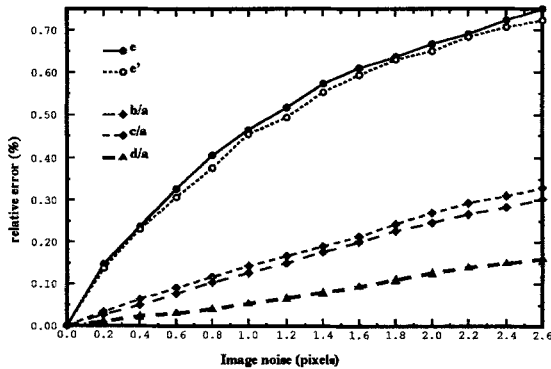


Fig. 1. Sensitivity to noise of the different components of the fundamental matrix

A relative distance [6], has been used to quantify the positional errors of the epipoles found. Since the four coefficients of the epipolar transformation are defined only up to a scale factor, we have normalized them by dividing by a , which allows to consider a relative error for each of them. From the results of the simulation shown Fig. 1, it is clear that:

- The stability of the epipoles in each of the images is comparable, which was to be expected, since the criterion (2) is symmetrical. Note that the non-linear criteria proposed in [6] also share this property.
- Once the epipoles are determined correctly, the computation of the homography is quite stable, and thus that the more unstable part of the computation is the determination of the epipoles.

We thus conclude from this simulation that *an adequate measure for the stability of the fundamental matrix is the stability of one of its epipoles*. Note that this is consistent with the findings of [8], where it has been shown that the epipole plays a particular role in the projective description of the geometry of a system of two cameras.

3 A Probabilistic Characterization

A classic characterization of uncertainty is to use covariance matrices. If the measurements are modeled by the random vector \mathbf{x} , of \mathbf{R}^P of mean \mathbf{x}_0 and of covariance $A_{\mathbf{x}} = E((\mathbf{x} - \mathbf{x}_0)^T(\mathbf{x} - \mathbf{x}_0))$, then the vector $\mathbf{y} = f(\mathbf{x})$ is a random vector whose first and second order moments can be expressed very simply, up to a first order approximation, as functions of the first and second order moments of \mathbf{x} . In effect, the mean is $f(\mathbf{x}_0)$ and the covariance matrix:

$$A_{\mathbf{y}} = \mathbf{J}_f(\mathbf{x}_0)A_{\mathbf{x}}\mathbf{J}_f(\mathbf{x}_0)^T \quad (5)$$

Where $\mathbf{J}_f(\mathbf{x}_0)$ is the Jacobian matrix of f , at the point \mathbf{x}_0 . In our case, the function f associates to the coordinates of the point correspondences the entries of the fundamental matrices eventually found. In the case of a linear criterion, already studied in [17] and [13] (for the computationally identical case of the essential matrix computed from the eight point algorithm), we have an explicit formula for the function f . A different approach is needed to cope with the case of a nonlinear criterion, since we do not have an explicit expression for f . We only know that f minimizes a known criterion, and this can be dealt with using a method based on the implicit functions theorem, presented in [1], and used for instance in [16]. Two examples, one with epipoles near the image center, the other with epipoles far away, are given in Fig. 2, where we have superimposed the uncertainty ellipses corresponding to a 90% probability, computed from the exact point coordinates, and the image frames.

A statistical test has then been performed using 200 configurations of points obtained by variation of cameras and 3D points. The correlation diagram between actual standard deviations (computed over 20 trials for each configuration) and predicted covariances (both from the exact point correspondences: light dots, and from the noisy point correspondences: dark dots), presented Fig. 3 shows that the correlation between the prediction and the actual covariances is quite high, even in case of prediction from the noisy data.

4 Ambiguity and the Critical Surface

Critical surfaces were known from the photogrameters of the beginning of the century, who called them "*gefährliche Flächen*". They were then rediscovered and studied theoretically by computer vision scientists in the case of reconstruction from optical flow [9] and point correspondences [4, 11, 2]. We are going to point out some *practical* consequences of the existence of such surfaces. Our approach is to provide algorithms which start from the data which is available to us in uncalibrated images, that is a set of point correspondences between two images. These algorithms provide us a practical means to quantify the proximity of the 3D points which have given rise to point correspondences, to such a critical surface, much the same way than the computation of an homography between projective coordinates of point correspondences [7] allowed us to assess the proximity of the 3D points to a plane.

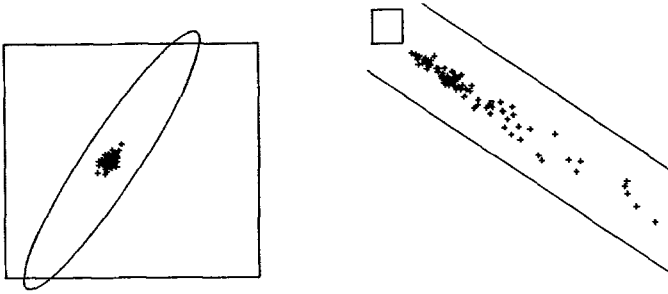


Fig. 2. Uncertainty ellipsis and noisy epipoles, left: first motion, right: second motion

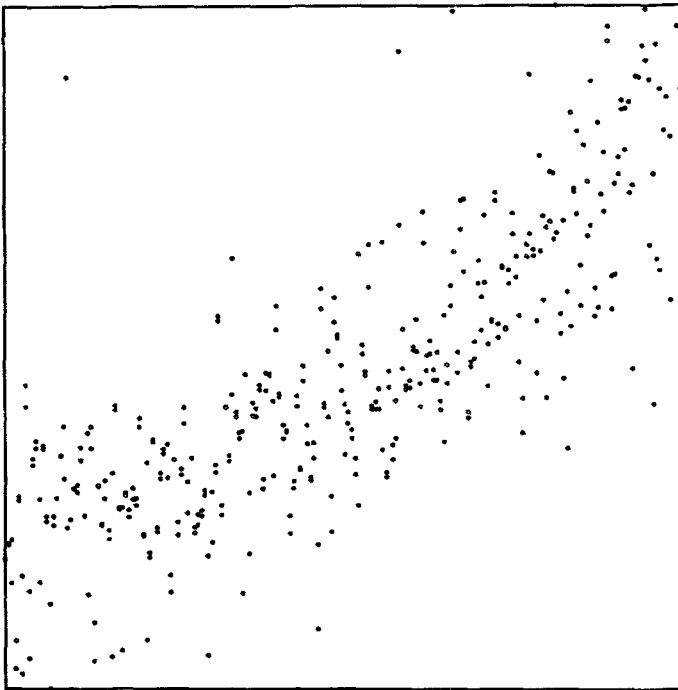


Fig. 3. Correlation between computed covariances and predicted covariances

The Critical Surface and Quadratic Transforms If all the observed points are in some special configuration, then the problem to obtain fundamental matrices from point correspondences may not have a unique solution, even with an arbitrarily large number of such correspondences. This happens when the measured points lie on some special surfaces called *critical surfaces* and yields several fundamental matrices compatible with the basic constraint : $\mathbf{m}'^T \mathbf{F} \mathbf{m} = 0$. Each of these fundamental matrices gives rise to a displacement which produces identical pairs of views, called *ambiguous*. More precisely, it is not possible to distinguish between the image of the set of 3D points Q_1 observed during displacement $\mathbf{R}_1, \mathbf{t}_1$, and the image of a set of points set

of 3D points Q_2 observed during displacement R_2, t_2 , as illustrated in Fig. 4. It has been shown [9] that the critical surfaces Q_1 and Q_2 are space quadrics containing the optical centers and the baseline of equations:

$$(R_1 M + t_1)^T E_2 M = 0 \quad (6)$$

$$(R_2 M + t_2)^T E_1 M = 0 \quad (7)$$

It is known that the maximum number of ambiguous fundamental matrices is three [4].

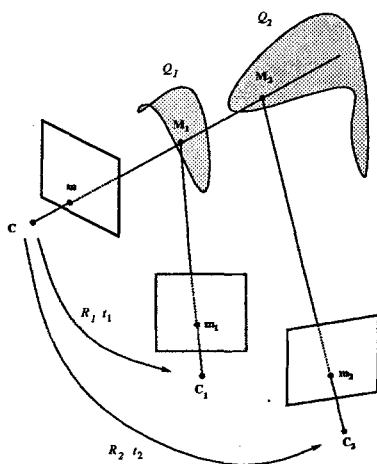


Fig. 4. Critical surfaces

Let us now characterize critical surfaces in terms of image quantities. Given two ambiguous images there exist two fundamental matrices F_1 and F_2 such that for each pair (m, m') of corresponding points,

$$m'^T F_1 m = 0 \quad \text{and} \quad m'^T F_2 m = 0$$

we can conclude from these two equations that:

$$m' = F_1 m \times F_2 m \quad (8)$$

This equation defines in general a *quadratic transformation* between the coordinates of the points in the two images. This is a generalization of the homography which we encountered and studied in the case of planes [7]. The quadratic transformation allows us to check if image points are close to the projection of a critical surface, much the same way as the homography allowed us to check if they were close to the projection of a plane. The epipoles of the three different fundamental matrices which are solutions to the problem, in an ambiguous situation, are the fundamental points of the quadratic transformation.

Quadratic transformations and their parameterizations Quadratic transformations are mappings of \mathcal{P}^2 into \mathcal{P}^2 , whose coordinates are homogeneous polynomials of degree 2, which are invertible, and whose inverse are also homogeneous polynomials of degree 2. The most simple example is the reciprocal transformation, defined by:

$$\Phi_0(\mathbf{x}) = (x_2x_3, x_3x_1, x_1x_2)^T$$

From this definition, we can see that Φ_0 is defined in each point of \mathcal{P}^2 , except for the points $\mathbf{i}_1 = (1, 0, 0)^T$, $\mathbf{i}_2 = (0, 1, 0)^T$ and $\mathbf{i}_3 = (0, 0, 1)^T$, which are called fundamental points of Φ_0 . We also notice that Φ_0 is invertible, since it is its own inverse.

In the general case, a quadratic transformation Φ has also three fundamental points $\mathbf{g}_1, \mathbf{g}_2, \mathbf{g}_3$ which are distinct of those of $\Phi^{-1}, \mathbf{g}'_1, \mathbf{g}'_2, \mathbf{g}'_3$. and we have:

$$\Phi = \mathbf{A}\Phi_0\mathbf{B} \tag{9}$$

where \mathbf{A} and \mathbf{B} are two collineations which can be interpreted as changes of retinal coordinates:

$$\begin{aligned} \mathbf{A}\mathbf{i}_1 &= \mathbf{g}'_1 & \mathbf{A}\mathbf{i}_2 &= \mathbf{g}'_2 & \mathbf{A}\mathbf{i}_3 &= \mathbf{g}'_3 & \mathbf{A}\mathbf{i}_4 &= \mathbf{g}'_4 \\ \mathbf{B}\mathbf{g}_1 &= \mathbf{i}_1 & \mathbf{B}\mathbf{g}_2 &= \mathbf{i}_2 & \mathbf{B}\mathbf{g}_3 &= \mathbf{i}_3 & \mathbf{B}\mathbf{g}_4 &= \mathbf{i}_4 \end{aligned} \tag{10}$$

where $\mathbf{i}_4 = (1, 1, 1)^T$. The inverse of Φ is $\Phi^{-1} = \mathbf{B}^{-1}\Phi_0\mathbf{A}^{-1}$. The point \mathbf{g}_4 can be chosen arbitrarily, whereas the point \mathbf{g}'_4 is determined by Φ [15]. Thus \mathbf{A} depends on 8 parameters (the projective coordinates of the points $\mathbf{g}'_i, i = 1, 2, 3, 4$) and \mathbf{B} depends on 6 parameters (the projective coordinates of the points $\mathbf{g}_i, i = 1, 2, 3$). Thus Φ depends on 14 parameters, which is consistent with (8), where Φ is defined by two fundamental matrices, which gives 7+7 parameters.

A first approach is to estimate the 14 parameters of the most general quadratic transformation Φ as given by (9) and (10). A second approach gives us only an *upper bound* of the distances of the points $(\mathbf{m}, \mathbf{m}')$ to the critical surface, but requires only the computation of 7 parameters. The idea is to start from a fundamental matrix \mathbf{F}_1 and to compute a second fundamental matrix \mathbf{F}_2 such that \mathbf{F}_1 and \mathbf{F}_2 define a quadratic transformation (8). For both approaches, we have designed a method consisting in a combination of the linear solution and non-linear minimization with an appropriate parameterization and symmetric Euclidean distance. Details can be found in [5].

Theoretical link between ambiguity and instability Critical surfaces have been presented in (4) as sets of points yielding ambiguous interpretations of motion. Maybank [11] has shown that a configuration whose 3D reconstruction is unstable is close to a critical surface. We are going to provide evidence for the reciprocal property.

The instability is very clear in the formulation of Horn [2] which defines critical surfaces as sets of points \mathbf{M} for which the variation of $\mathbf{m}'^T\mathbf{E}\mathbf{m}$ is a second-order (quadratic) function of the parameters \mathbf{r}, \mathbf{t} . While the equation he obtains is quite different from (7), he finds properties similar to the one which are described by Maybank [10]. We are going to see that the two forms are indeed equivalent, which will prove that an ambiguous situation is also unstable.

Normalized coordinates are used, the optical center \mathbf{C} being mapped onto the optical center \mathbf{C}' by the displacement \mathbf{R}, \mathbf{t} , perturbed by the infinitesimal vectors $\delta\mathbf{r}, \delta\mathbf{t}$. The difference of residual values of the Longuet-Higgins equation for unperturbed and perturbed displacement can be expressed in the final coordinate system, using triple products, as:

$$\Delta = [(\mathbf{t} + \delta\mathbf{t}), \mathbf{C}'\mathbf{M}, \mathbf{C}\mathbf{M} + \delta\mathbf{r} \times \mathbf{C}\mathbf{M}] - [\mathbf{t}, \mathbf{C}'\mathbf{M}, \mathbf{C}\mathbf{M}] \tag{11}$$

We have used the fact that an infinitesimal rotation $\delta\mathbf{R}$ can be expressed from $\delta\mathbf{r}$ using the Rodrigues formula, with an infinitesimal $\theta = \|\delta\mathbf{r}\|$:

$$\delta\mathbf{R} = e^{\tilde{\delta\mathbf{r}}} = \mathbf{I} + \frac{\sin\theta}{\theta}\tilde{\delta\mathbf{r}} + \frac{1 - \cos\theta}{\theta^2}\tilde{\delta\mathbf{r}}^2 \sim \mathbf{I} + \tilde{\delta\mathbf{r}}$$

The difference Δ in (11) is normally a first order quantity, and the unstable situations are those for which it is a higher order quantity. If we drop the second order term $[\delta\mathbf{t}, \mathbf{C}'\mathbf{M}, \delta\mathbf{r} \times \mathbf{C}\mathbf{M}]$ we obtain by expanding the products:

$$\Delta = [\mathbf{t}, \mathbf{C}'\mathbf{M}, \delta\mathbf{r} \times \mathbf{C}\mathbf{M}] + [\delta\mathbf{t}, \mathbf{C}'\mathbf{M}, \mathbf{C}\mathbf{M}]$$

Using $\mathbf{t} = \mathbf{C}'\mathbf{C}$ and some standard properties of the triple product yields:

$$\Delta = [(\mathbf{I} + \tilde{\delta\mathbf{r}})\mathbf{C}'\mathbf{M} - \delta\mathbf{r} \times \mathbf{t} + \delta\mathbf{t}, \mathbf{t}, \mathbf{C}'\mathbf{M}]$$

It is easy to see that this is equivalent to Horn's expression. Now using \mathbf{M} in the initial coordinate system, we obtain, by writing that the triple product is zero:

$$((\mathbf{I} + \tilde{\delta\mathbf{r}})\mathbf{R}\mathbf{M} - \delta\mathbf{r} \times \mathbf{t} + \delta\mathbf{t})^T(\mathbf{t} \times \mathbf{R}\mathbf{M}) = 0 \quad (12)$$

A critical surface given by (7), can be written in the initial coordinate system:

$$(\mathbf{R}_2\mathbf{M} + \mathbf{t}_2)^T(\mathbf{t} \times \mathbf{R}\mathbf{M}) = 0$$

which is has the form (12).

5 Experimental Results

The Nature of the Motion Since the epipoles are a simple function of the camera displacement, we can expect that the stability of the fundamental matrix computation can be related to the stability of motion estimation [17] We have studied three cases where the results are unstable:

- small translational component,
- translational component parallel to the image plane³
- pure translation.

Extensive experimental simulations and qualitative explanations can be found in [5].

An Experiment Starting from a Critical Surface In order to show that critical surfaces are a cause of instability, we first start from 3D points that are generated on such a surface \mathcal{Q} . We then construct different sets \mathcal{Q}_d of 3D points which lie close to the critical surface. Each point $\mathbf{M}_i(d)$ is obtained from the point \mathbf{M}_i of the surface \mathcal{Q} from $\mathbf{M}_i \pm d\mathbf{n}_i$, where \mathbf{n}_i is the unit normal to the surface \mathcal{Q} at \mathbf{M}_i , and d is a fixed scalar which represents the 3D distance of \mathcal{Q}_d to \mathcal{Q} . Taking the \mathcal{Q}_d instead of the \mathcal{Q} amounts to "add noise to the critical surface", in order to assess the "robustness of instability", or to evaluate the "critical volume". To assess the stability of fundamental matrix computation, we have then estimated the variance of the coordinates of the epipoles from 50 tries, for different values of the distance to the critical surface and the image noise. The results appear in Table 1, where we also show the mean values d_x and d_y of the retinal disparities between the projections of points of \mathcal{Q} and the projections of the corresponding points of \mathcal{Q}_d .

³ The epipoles are far from the image center.

Table 1. Influence of the distance to the critical surface and of image noise on the stability.

d	d_x	d_y	$b = 0$		$b = 0.5$		$b = 1$	
			σ_{e_x}	σ_{e_y}	σ_{e_x}	σ_{e_y}	σ_{e_x}	σ_{e_y}
0	0	0	6140	3639	1466	872	1261	788
5	3.89	7.74	10^{-7}	10^{-7}	2935	1765	3749	2305
10	7.60	14.51	10^{-7}	10^{-7}	726.	459	822	492
20	15.19	29.12	10^{-7}	10^{-7}	153	106	280	199
50	89.34	148.53	10^{-7}	10^{-7}	39	40	65	68

Let us comment the results. First, it is clear that the farther the points are from the critical surface, the more stable are the results. When the points are far away from the critical surface, an increase of the image noise increases the covariance of the epipoles, which is to be expected, but when they are very close to the critical surface, the noise induces a reconstruction error which drives the points away from the critical surface, which explains why the variances decrease a little. If there is no image noise, then 3D points are reconstructed exactly. In this case, their 3D distance to the critical surface, even if it is very small, is significant, and unstability does not occur. In the case where there is some image noise, the 3D points are reconstructed with an uncertainty. Now if the original 3D points were close to the critical surface, and if this distance is smaller than the reconstruction uncertainty, then they cannot be distinguished from points lying on the critical surface, and thus unstability will occur. Thus, the volume for which unstability occurs depends on the 2D noise and we call it the *critical volume*.

A Global Experiment So far, we have always started from synthetic data which was created to illustrate some facts. Now we start from the image data, such that it would be available to an algorithm, and we try to explain the sources of uncertainty. This experiment was carried on using synthetic data because at that time we did not have a reliable system to obtain automatically point matches, but the principle would be exactly the same with real data. In this experiment, we try to account simultaneously for two sources of unstability, the proximity to a critical surface, and the distance of the epipole to the image center. Note that we have eliminated data with small retinal disparity in order to ignore the unstability due to small and pure translations. The image noise is 2 pixels. For each of the 500 displacements, we have computed the epipoles and their covariance matrices, and ordered the trials by increasing unstability. The horizontal axis in Fig. 5 represents unstability increasing from left to right.

We have first considered the distance of the epipole to the image center, represented on the Y-axis. There is a correlation between this distance, and unstability, quantified by the leftmost and rightmost columns of Table 2.

The next idea is to try to fit a critical surface, by computing the reprojected distance to a critical surface using the method described in Sect. 4. Since the 3D points are chosen randomly, their probability to lie on a critical surface is almost zero. However, and this is one of our findings, they may lie *near* a critical surface, which means that they are in a critical volume. The idea is, after estimating the fundamental matrix F_1 from the point correspondences, to find the fundamental matrix F_2 which minimizes (8). This is like trying to fit a critical surface to the 3D points which have

Table 2. Sources of instability in a statistical experiment.

displacements (increasing instability)	critical surface at less than 10 pixels	average distance of epipoles to image center
1-100	9%	754.6 pixels
101-200	13%	1164 pixels
201-300	31%	1783 pixels
301-400	40%	2624 pixels
401-500	49%	25280 pixels

given rise to the point correspondences. If the residual distance, which is the value of the criterion (8) at the minimum, is high, it means that no fit can be found, and thus the critical surface does not exist. But if the residual is low, it means that the 2D points lie near the projection of a critical surface, the distance of the points to the projection of the fitting critical surface being given by the residual. Of course, there is a continuum of possibilities, and we have chosen the threshold of 10 pixels, for which we know that instability is still significant, as shown by the example presented in Table 1.

The black dots in Fig. 5 are those for which the distance is under the threshold. Let us consider two points N_1 and N_2 in Fig. 5, with approximately the same horizontal coordinate, but for which the vertical coordinates are different, say $y_1 > y_2$. The points have the same stability, but N_2 correspond to a motion yielding an epipole which is closer to the image center than N_1 . The reason may be that N_2 represents a configuration which is close to a critical surface. Now we can notice that these points (the dark dots) are statistically below the light dots (corresponding to distances to the critical surface which are more than 10 pixels), which validate this hypothesis. Another thing which may be observed is that there are more black dots in the area of high instability (right), as shown in the middle column of Table 2 as well as in Fig. 5. Thus, the combination of the proximity to a critical surface and the direction of translation provides a better explanation for instability than any of these two causes in isolation.

Another important observation is the omnipresence of the critical surface, which is at less than 10 pixels in 28% of the displacements. Although the critical surfaces do not exist *exactly* in normal scenes in the sense that real objects rarely are critical surface, they have a large practical importance since our experiments show that the *critical volume* where the points have to lie in order to yield some instability is rather large.

6 Conclusion

In this paper, we have studied the influence of the camera motion on the stability of the fundamental matrix. Two tools have been introduced, a probabilistic characterization of stability via computation of covariance matrices, and a method to estimate the reprojection distance to the closest critical surface from image data via computation of a quadratic transformation. Using these tools we have been able to characterize the unstable situations. They can result from the nature of the motion (situations

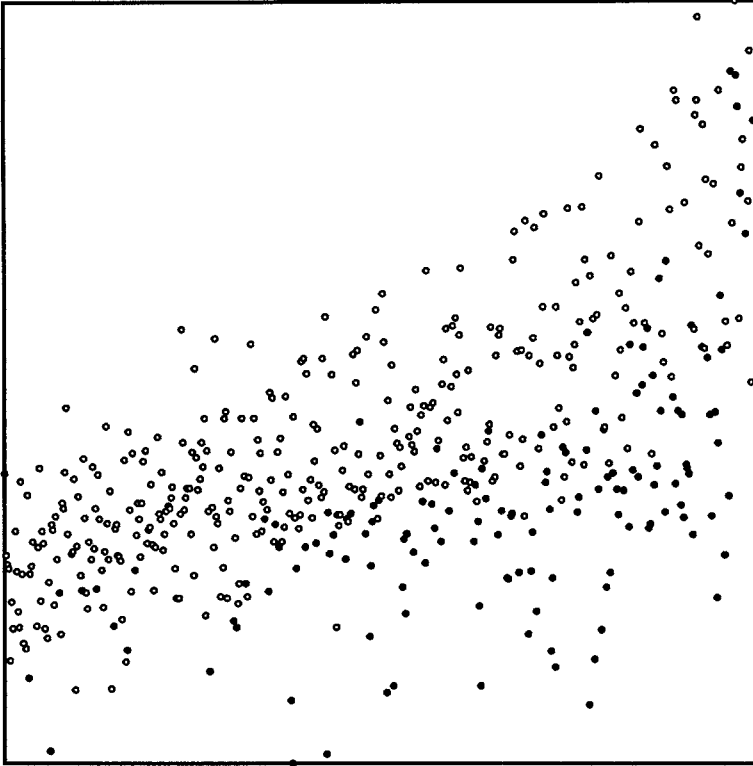


Fig. 5. A global experiment to characterize the causes of instability (see text)

we have identified are small translational components, large translational component parallel to the image plane, and pure translations), but also in a more subtle way, from the interaction of the camera motion and the 3D structure of the scene, which can be described by a critical surface. These characterizations have been validated experimentally through statistical simulations. Some of the new results which have been found are also applicable to the problem of Euclidean motion stability analysis. They suggest that surprisingly enough, the critical surface, apparently a mostly theoretical construction, affects the stability of the fundamental matrix in a significant number of situations.

Acknowledgements

We would like to thank Steve Maybank and Nassir Navab for fruitful discussions during the progress of this work. QTL was supported by an INRIA doctoral grant.

References

1. O.D. Faugeras. *Three-dimensional computer vision: a geometric viewpoint*. MIT Press, 1993. To appear.

2. B.K.P. Horn. Relative orientation. *The International Journal of Computer Vision*, 4(1):59–78, Jan. 1990.
3. H.C. Longuet-Higgins. A Computer Algorithm for Reconstructing a Scene from Two Projections. *Nature*, 293:133–135, 1981.
4. H.C. Longuet-Higgins. Multiple interpretations of a pair of images of a surface. *Proc. of the Royal Society London A*, 418:1–15, 1988.
5. Q.-T. Luong. *Matrice fondamentale et auto-calibration en vision par ordinateur*. PhD thesis, Universite de Paris-Sud, Orsay, Dec. 1992.
6. Q.-T. Luong, R. Deriche, O.D. Faugeras, and T. Papadopoulos. On determining the Fundamental matrix: analysis of different methods and experimental results. Technical Report RR-1894, INRIA, 1993. A shorter version appeared in the Israelian Conf. on Artificial Intelligence and Computer Vision.
7. Q.-T. Luong and O.D. Faugeras. Determining the Fundamental matrix with planes: unstability and new algorithms. In *Proc. Conference on Computer Vision and Pattern Recognition*, pages 489–494, New-York, 1993.
8. Q.-T. Luong and T. Viéville. Canonic representations for the geometries of multiple projective views. Technical Report UCB/CSD-93-772, University of California at Berkeley, Sept 1993. Accepted at ECCV'94.
9. S.J. Maybank. The angular velocity associated with the optical flow field arising from motion through a rigid environment. *Proc. of the Royal Society London A*, 401:317–326, 1985.
10. S.J. Maybank. The projective geometry of ambiguous surfaces. *Proc. of the Royal Society London A*, 332:1–47, 1990.
11. S.J. Maybank. Properties of essential matrices. *International journal of imaging systems and technology*, 2:380–384, 1990.
12. J. L. Mundy and A. Zisserman, editors. *Geometric invariance in computer vision*. MIT Press, 1992.
13. J. Philip. Estimation of three-dimensional motion of rigid objects from noisy observations. *IEEE Transactions on Pattern Analysis and Machine Intelligence*, 13(1):61–66, 1991.
14. L. Quan. Affine stereo calibration for relative affine shape reconstruction. In *Proc. British Machine Vision Conf.*, 1993.
15. J.G. Semple and G.T. Kneebone. *Algebraic Projective Geometry*. Oxford: Clarendon Press, 1952. Reprinted 1979.
16. T. Viéville and P. Sander. Using pseudo kalman-filters in the presence of constraints. Technical Report RR-1669, INRIA, 1992.
17. J. Weng, T.S. Huang, and N. Ahuja. Motion and structure from two perspective views: algorithms, error analysis and error estimation. *IEEE Transactions on Pattern Analysis and Machine Intelligence*, 11(5):451–476, 1989.